Volume 354, Nos. 12–13, 15 February 2008

ISSN 0022-3093

ELSEVIER

# JOURNAL OF NON-CRYSTALLINE SOLIDS



## 2005 INTERNATIONAL SYMPOSIUM ON GLASS

Proceedings of the 2005 International Conference on Glass
(in conjunction with the Annual Meeting of the International Commission on Glass)

Shanghai, China, 10–14 April 2005

*Guest Editors:*
F. Gan, A.C. Wright, C. Zhu

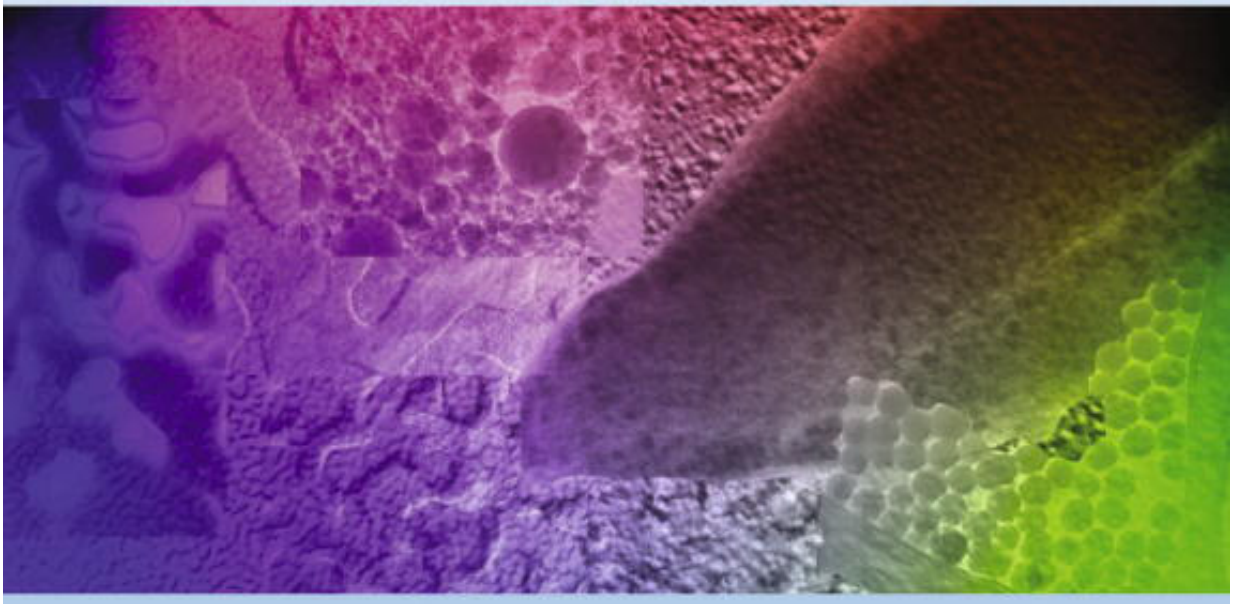

Available online at www.sciencedirect.com
ScienceDirect
Journal of Non-Crystalline Solids 354 (2008) 1240–1244
JOURNAL OF NON-CRYSTALLINE SOLIDS
www.elsevier.com/locate/jnoncrysol

# Glass nanofibers for micro- and nano-scale photonic devices

Limin Tong [a,b,*], Eric Mazur [b]

[a] State Key Laboratory of Modern Optical Instrumentation, Zhejiang University, Hangzhou 310027, China
[b] Department of Physics and Division of Engineering and Applied Sciences, Harvard University, Cambridge, MA 02138, USA

**Abstract**

Subwavelength- and nanometer-diameter glass nanofibers have been fabricated using a high-temperature taper-drawing process. As-drawn nanofibers show extraordinary uniformities in terms of diameter variation and surface roughness and are suitable for single-mode optical wave guiding. Measured optical losses of these nanofibers are typically below 0.1 dB/mm. Photonic devices such as linear waveguides, optical couplers and microrings assembled with nanofibers are also demonstrated. Our results show that taper-drawn glass nanofibers are promising building blocks for micro- and nano-scale photonic devices.


*PACS:* 42.79.Gn; 81.16.–c

*Keywords:* Fibers and waveguides; Optical fibers; Optical properties; Silica

## 1. Introduction

Glass, one of the fundamental materials for photonics, can readily be shaped into macro- or micro-scale optical components such as lenses, prisms and fibers that are widely used in optical communications, sensors and other applications [1–3]. Future micro- and nano-scale photonic devices are likely to demand further miniaturization of the size of the glass-based photonic components. Here we show that optical-quality glass nanofibers with diameters ranging from tens to hundreds of nanometers can be obtained using a simple, high-temperature taper-drawing technique. Because of their excellent diameter uniformities and atomic-level surface smoothness, glass nanofibers can be used as subwavelength-diameter single-mode waveguides with low optical losses. Using high-precision nano-manipulation, these nanofibers can be assembled into various micro- and nano-scale photonic devices.

* Corresponding author. Address: State Key Laboratory of Modern Optical Instrumentation, Zhejiang University, Hangzhou 310027, China. Tel./fax: +86 571 87967187.
*E-mail address:* phytong@zju.edu.cn (L. Tong).

0022-3093/$ - see front matter © 2007 Elsevier B.V. All rights reserved.
doi:10.1016/j.jnoncrysol.2006.10.090

## 2. Fabrication of glass nanofibers

Glass nanofibers are fabricated using a high-temperature taper-drawing technique. To draw a nanofiber with diameter below 200 nm, we use a two-step taper-drawing method [4]. First, we use a flame or carbon oxide laser beam to draw a standard glass fiber (e.g., SMF28, Corning Inc.) to a micrometer-diameter fiber taper. Second, to further reduce the fiber diameter and maintain a steady temperature distribution in the drawing region, we use a tapered sapphire fiber of about 100 μm in diameter to absorb the flame energy and generate an appropriate temperature distribution. As illustrated in Fig. 1, after the flame is adjusted so that the temperature of the sapphire tip is a bit higher than the drawing temperature (about 2000 K), we place one end of a micrometer-diameter fiber horizontally on the sapphire tip and rotate the tip around its axis of symmetry so as to wind the microfiber around it. Then we draw the fiber perpendicular to the axis of the sapphire tip in the horizontal plane at a speed of 1–10 mm/s to form the nanofiber. When the drawing is completed, the nanofiber is connected to the starting fiber at one end and free-standing on the other end. We use a homemade $CH_3OH$ torch burning in air with a

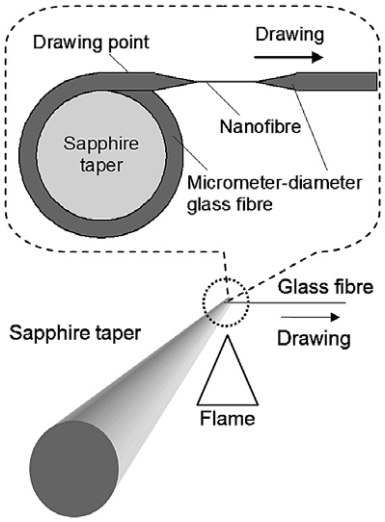


Fig. 1. Schematic diagram of the second-step taper-drawing of nanofibers with assistance of a sapphire taper.

nozzle-diameter of about 6 mm. Because the working temperature is below the melting temperature of sapphire (about 2320 K), the sapphire tip can be used repeatedly.

Using this technique, we obtained long glass nanofibers with diameters down to 50 nm (very recently, nanofibers as thin as 20 nm have been obtained using a self-modulated taper-drawing process [5]). Generally, the nanofiber starts from a tapered transition region connected to the starting microfiber with a length of millimeters. The main part of the fiber, with a length from hundreds of micrometers to tens of millimeters, has excellent diameter uniformity and surface smoothness. Fig. 2(a) shows scanning electron microscope (SEM) images of a glass nanofiber with a uniform diameter of 260 nm. The nanofiber is placed on a 5.8-μm-diameter microfiber from which it is drawn. Fig. 2(b) shows a SEM image of the circular cross-section of a 480-nm-diameter nanofiber. The cylindrical geometry of the fibers makes it possible to obtain their guiding modes by solving Maxwell's equations analytically [6]. The sidewall roughness of the nanofibers is investigated using transmission electron microscopy (TEM). Fig. 2(c) gives a typical TEM image of the sidewall of a 220-nm-diameter glass nanofiber. The electron diffraction pattern shown in the inset indicates that the nanofiber is amorphous. The typical sidewall root mean square (RMS) roughness is less than 0.3 nm, much lower than those of submicrometer wide wires, strips or similar structures obtained using other fabrication methods [7–9]. Considering that the length of Si–O bond is about 0.16 nm [10], such a roughness indicates an atomic-level smoothness of the nanofiber surface.

## 3. Optical wave guiding properties of glass nanofibers

The optical wave guiding behavior of these subwavelength diameter nanofibers can be obtained by numerically solving Maxwell's equations [11]. Fig. 3(a) shows the normalized propagation constant (effective index) $\beta/k_0$, where $\beta$ is the propagation constant and $k_0 = 2\pi/\lambda_0$, of the first four modes in air-clad silica nanofibers. When the normalized fiber diameter $D/\lambda_0$ falls below 0.73, the fiber is a single-mode waveguide. Fig. 3(b) shows the fractional power of the fundamental mode ($HE_{11}$) inside the glass core at

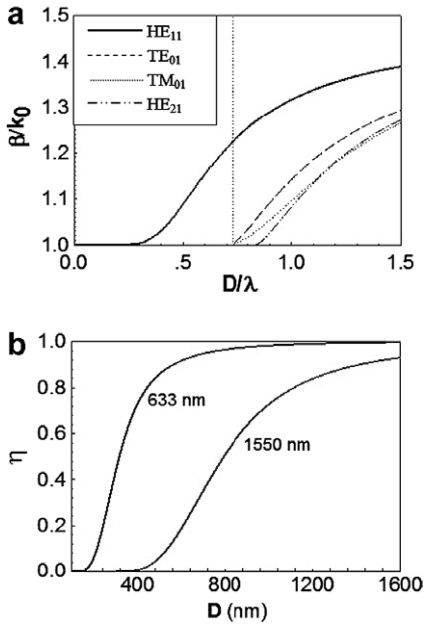


Fig. 3. Optical wave guiding properties of air-clad glass nanofibers. (a) Normalized propagation constants $\beta/k_0$ for the first four modes. The dotted line indicates the single-mode cut-off condition. (b) Fractional power of the $HE_{11}$ mode inside the core at wavelengths of 633 and 1550 nm.

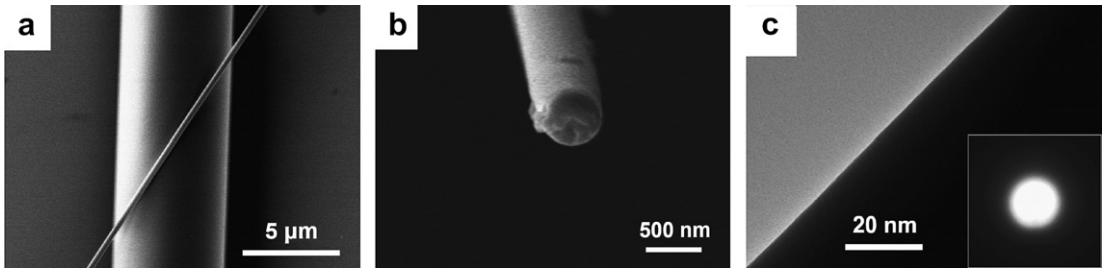


Fig. 2. Electron microscope images of glass nanofibers. (a) SEM image of a 260-nm-diameter nanofiber placed on a 5.8-μm-diameter microfiber. (b) SEM image of the cross-section of a 480-nm-diameter nanofiber. (c) TEM image of the edge of a 220-nm-diameter nanofiber. Inset: electron diffraction pattern.

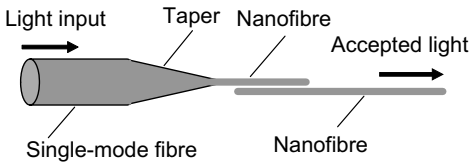


Fig. 4. Schematic diagram of launching light from a fiber taper into a glass nanofiber by means of evanescently coupling.

two typical wavelengths (633 and 1550 nm). For example, at the single-mode cut-off diameter ($D_{SM}$), more than 80% of the light energy is confined inside the fiber, demonstrating its tight-confinement ability. When the fiber diameter is reduced to $0.5D_{SM}$ (e.g., 229 nm for light of 633-nm wavelength), about 86% of the light power propagates outside the fiber as an evanescent wave. Tight confinement reduces bending losses in sharp bends. Weak confinement, on the other hand, facilitates light coupling from one fiber to another, and is advantageous for high-sensitivity optical sensing [12–14].

To experimentally investigate the guiding properties of the glass nanofibers, we send light into them using an evanescent coupling method as shown in Fig. 4. Light is first sent into the core of a single-mode fiber that is tapered down to a nanofiber and this nanofiber is then used to evanescently couple the light into another one by overlapping the two in parallel. Because of electrostatic and van der Waals forces nanofibers attract one another, making a contact connection. The coupling efficiency of this evanescent coupling can be as high as 90% when the fiber diameter and overlap length are properly selected. Because of the nanofibers' extraordinary uniformity, the optical loss of these nanofibers is extremely low. Typical optical loss measured at $D_{SM}$ (e.g., about 1100 nm at a wavelength of 1550 nm) is below 0.1 dB/mm [4], and has recently been further reduced to be below 0.01 dB/mm [15,16], which is much lower than the optical loss of other subwavelength-structures such as metallic plasmon waveguides or nanowires fabricated by many other methods such as electron beam lithography or chemical growth [17–19].

## 4. Glass nanofibers for micro- and nano-scale photonic devices

Because of their long length, glass nanofibers obtained by the taper-drawing method can easily be seen under an optical microscope. This optical visibility makes it possible to manipulate the nanofibers in air, greatly facilitating the handling and assembly of these nanofibers. Also, because of their excellent uniformity, these fibers have high mechanical strength and pliability; using probes from a scanning tunneling microscope (STM) to hold and manipulate the fibers under an optical microscope, we have assembled glass nanofibers into various patterns.

To support the nanofiber waveguides for device integration, we use silica aerogel as a low-index non-dissipative substrate. Silica aerogel is a tenuous porous silica network of silica nanoparticles about 30 nm in size, much smaller than the wavelength of the guided light, and has a transparent optical spectral range similar to that of silica [20,21]. Because the aerogel is mostly air, its refractive index (about 1.03 at a wavelength of 633 nm) is very close to that of air. Fig. 5(a) shows a close-up view of a glass nanofiber of 530-nm-diameter supported on a substrate of silica aerogel. Because the index difference between the silica aerogel and air (about 0.03) is much lower than the index difference between the silica nanofiber and air (about 0.45), the optical guiding properties of aerogel-supported fibers are virtually identical to those of the air-clad fibers discussed in Section 3 (see Fig. 3).

The aerogel-supported nanofiber guides light with low optical loss. Fig. 5(b) shows a glass nanofiber of 360-nm-diameter guiding light of 633-nm wavelength on the surface of a silica aerogel substrate. The uniform scattering along the length of the fiber and the strong output at the end of the nanofiber indicate that the optical loss of guided light is low. For glass nanofibers with a diameter around $D_{SM}$, the measured optical loss of aerogel-supported nanofibers is typically less than 0.06 dB/mm [22], which is low enough for building micro- or nanophotonic devices.

To make a waveguide bend, we first anneal an elastically bent fiber on the surface of a sapphire substrate, and then transfer it to silica aerogel. The measured bending loss of a 5-μm-radius bend assembled with a 550-nm-diameter glass nanofiber is typically less than 1 dB at 633-nm wavelength, which is small enough for microphotonic circuits. By comparison, bending waveguides based on planar photonic crystal structures not only require multiple periods (which increase the overall size) and sophisticated fabrication techniques [23–25], but they also have inevitable out-of-plane loss. In contrast, aerogel-supported nanofiber bends offer the advantages of compact overall size, low loss, simple structure and easy fabrication [26]. In addition, unlike wavelength-specific photonic crystal structures, nanofiber bends can be used over a broad range of wavelengths, from the near-infrared to ultraviolet wavelengths.

Using waveguide bends as building blocks, one can readily assemble photonic devices such as optical couplers and microrings. Fig. 5(c), for example, shows a branch coupler assembled from two glass nanofibers of 450-nm-diameter. When light of 633-nm wavelength is launched into the bottom left arm, the coupler splits the flow of light into two. With an overlap of less than 5 μm, the device works as a 30/70 splitter. Microscopic couplers such as fused couplers, made from fiber tapers using conventional methods, require an interaction length on the order of 100 μm [27]. By comparison, couplers assembled with glass nanofibers reduce the device size by more than an order of magnitude. Shown in Fig. 5(d) is a 150-μm-diameter ring assembled with an 880-nm-diameter nanofiber. Measured transmittance of this microring around the wavelength of 1.55 μm is shown in Fig. 5, from which one sees clearly the optical interference effect. Such a ring can be used to spectrally

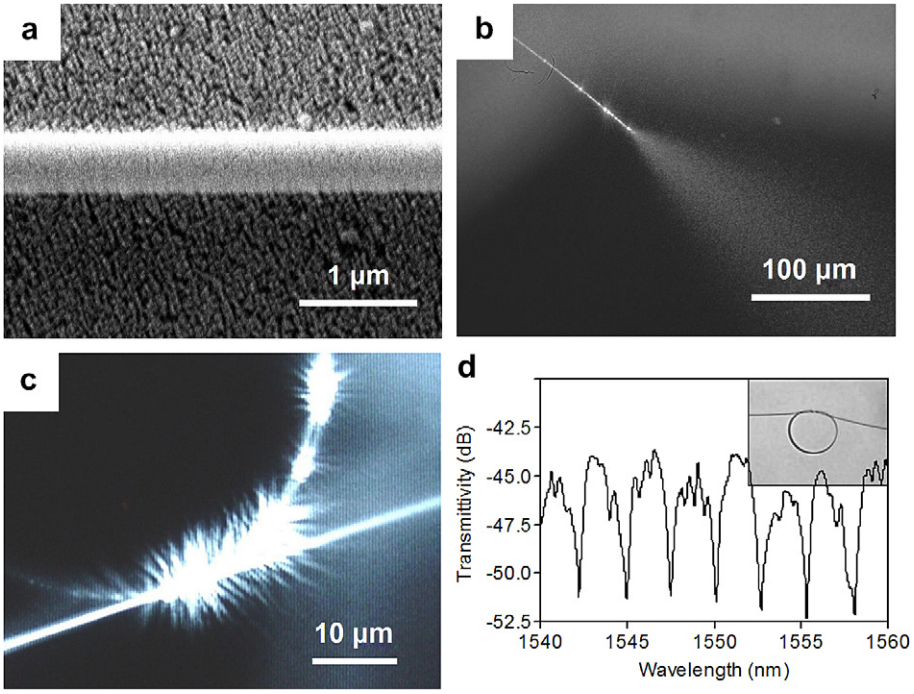


Fig. 5. Assembly of glass nanofibers on silica aerogel for micro- and nano-scale photonic devices. (a) A close-up view of a 530-nm-diameter nanofiber supported by silica aerogel substrate. (b) An aerogel-supported 360-nm-diameter nanofiber guiding light and output on the surface of silica aerogel. (c) A branch coupler assembled from two 450-nm-diameter nanofibers splits a 633-nm-wavelength light. (d) Transmission spectrum of a microring assembled with an 880-nm-diameter nanofiber. Inset, optical microscope image of the microring with a diameter of about 150 μm.

modulate a light signal, and may be developed to various photonic devices such as microring resonators as have been reported recently [28–30].

Beyond the photonic devices mentioned above, glass nanofibers have also inspired broad interest in other fields such as nonlinear interaction and supercontinuum generation [16,31–38], optical sensing [12–14], and atom trapping and guidance [39–42].

## 5. Conclusions

In conclusion, glass nanofibers can be fabricated by high-temperature taper- drawing technique. These nanofibers show excellent diameter uniformity and surface smoothness for low-loss optical wave guiding, making them promising building blocks for micro- and nano-scale photonic devices.

## Acknowledgments

This work is supported by the National Natural Science Foundation of China (Nos. 60425517 and 60378036) and the US National Science Foundation (PHY-9988123). Limin Tong acknowledges support from the Center for Imaging and Mesoscale Structures at Harvard University. We thank Albert Tsao for proofreading of this article.

## References

[1] K. Hirao, T. Mitsuyu, J. Si, J. Qiu, Active Glass for Photonic Devices: Photoinduced Structures and their Applications, Springer, New York, 2001.
[2] M. Yamane, Y. Asahara, Glasses for Photonics, Cambridge University, Cambridge, 2000.
[3] H. Murata, Handbook of Optical Fibers and Cables, Marcel Dekker, New York, 1996.
[4] L. Tong, R.R. Gattass, J.B. Ashcom, et al., Nature 426 (2003) 816.
[5] L. Tong, J. Lou, Z. Ye, G.T. Svacha, E. Mazur, Nanotechnology 16 (2005) 1445.
[6] A.W. Snyder, J.D. Love, Optical Waveguide Theory, Chapman and Hall, New York, 1983.
[7] Z.W. Pan, Z.R. Dai, C. Ma, Z.L. Wang, J. Am. Chem. Soc. 124 (2002) 1817.
[8] Y. Xia, J.A. Rogers, K.E. Paul, G.M. Whitesides, Chem. Rev. 99 (1999) 1823.
[9] K.K. Lee, D.R. Lim, L.C. Kimerling, J. Shin, F. Cerrina, Opt. Lett. 26 (2001) 1888.
[10] N.P. Bansal, R.H. Doremus, Handbook of Glass Properties, Academic Press, Orlando, 1986.
[11] L. Tong, J. Lou, E. Mazur, Opt. Exp. 12 (2004) 1025.
[12] J. Lou, L. Tong, Z. Ye, Opt. Exp. 13 (2005) 2135.
[13] P. Polynkin, A. Polynkin, N. Peyghambarian, M. Mansuripur, Opt. Lett. 30 (2005) 1273.
[14] J. Villatoro, D. Monzón-Hernández, Opt. Exp. 13 (2005) 5087.
[15] G. Brambilla, V. Finazzi, D.J. Richardson, Opt. Express 12 (2004) 2258.
[16] S.G. Leon-Saval, T.A. Birks, W.J. Wadsworth, P.St.J. Russell, M.W. Mason, Opt. Exp. 12 (2004) 2864.
[17] J. Takahara, S. Yamagishi, H. Taki, A. Morimoto, T. Kobayashi, Opt. Lett. 22 (1997) 475.
[18] S.A. Maier, P.G. Kik, H.A. Atwater, Appl. Phys. Lett. 81 (2002) 1714.

[19] C.J. Barrelet, A.B. Greytak, C.M. Lieber, NanoLetters 4 (2004) 1981.
[20] A.C. Pierre, G.M. Pajonk, Chem. Rev. 102 (2002) 4243.
[21] Y.K. Akimov, Instrum. Exp. Technol. 46 (2003) 287.
[22] L. Tong, J. Lou, R.R. Gattass, et al., NanoLetters 5 (2005) 259.
[23] J.D. Joannopoulos, R.D. Meade, J.N. Winn, Photonic Crystals: Molding the Flow of Light, Princeton University Press, Princeton, 1995.
[24] J. Moosburger, M. Kamp, A. Forchel, et al., Appl. Phys. Lett. 79 (2001) 3579.
[25] M. Augustin, H.J. Fuchs, D. Schelle, et al., Appl. Phys. Lett. 84 (2004) 663.
[26] P. Domachuk, B.J. Eggleton, Nat. Mater. 3 (2004) 85.
[27] G. Kakarantzas, T.E. Dimmick, T.A. Birks, R. Le Roux, P.St.J. Rusell, Opt. Lett. 26 (2001) 1137.
[28] M. Sumetsky, Opt. Exp. 12 (2004) 2303.
[29] M. Sumetsky, Y. Dulashko, J.M. Fini, A. Hale, Appl. Phys. Lett. 86 (2005) 161108.
[30] M. Sumetsky, Opt. Exp. 13 (2005) 4331.
[31] M.A. Foster, K.D. Moll, A.L. Gaeta, Opt. Exp. 12 (2004) 2880.
[32] Y.K. Lize, E.C. Magi, V.G. Ta'eed, J.A. Bolger, P. Steinvurzel, B.J. Eggleton, Opt. Exp. 12 (2004) 3209.
[33] M. Kolesik, E.M. Wright, J.V. Moloney, Appl. Phys. B 79 (2004) 293.
[34] E.C. Magi, H.C. Nguyen, B.J. Eggleton, Opt. Exp. 13 (2005) 453.
[35] J.M. Moison, A.M. Apetrei, J.A. Levenson, G. Melin, P. Pedeboscq, A. Fleureau, S. Lempereur, L. Gasca, Opt. Exp. 13 (2005) 1193.
[36] G. Brambilla, E. Koizumi, X. Feng, D.J. Richardson, Electron. Lett. 41 (2005) 400.
[37] D.K. Qing, G. Chen, Phys. Rev. B 71 (2005) 153107.
[38] A. Zheltikov, J. Opt. Soc. Am. B 22 (2005) 1100.
[39] F. Le Kien, V.I. Balykin, K. Hakuta, J. Phys. Soc. Jpn. 74 (2005) 910.
[40] F. Le Kien, V.I. Balykin, K. Hakuta, Phys. Rev. A 70 (2004) 063403.
[41] F. Le Kien, J.Q. Liang, K. Hakuta, V.I. Balykin, Opt. Commun. 242 (2004) 445.
[42] V.I. Balykin, K. Hakuta, F. Le Kien, J.Q. Liang, M. Morinaga, Phys. Rev. A 70 (2004) 011401.